Applied Energy 265 (2020) 114820

Contents lists available at ScienceDirect

Applied Energy

journal homepage: www.elsevier.com/locate/apenergy

Optimal control of flexible natural gas combined cycles with stress monitoring: Linear vs nonlinear model predictive control☆

Jairo Rúa*, Lars O. Nord

Department of Energy and Process Engineering, Norwegian University of Science and Technology, Trondheim, Norway

HIGHLIGHTS

- Maximum gas turbine load gradient is the main limitation during load changes
- Linear MPC shows superior performance than nonlinear MPC
- Possible to resort to nonlinear MPC when linear stress modelling is not feasible
- Proposed control methodology is able to predict stresses in thick-walled components
- Stress monitoring allows optimal and safe control sequences under tight constraints

ARTICLE INFO

Keywords:
Optimal control strategy
Thermal and mechanical stress
Linear and nonlinear MPC
Gas turbine combined cycle
Dynamic modelling and simulation
Dynamic flexible operation

ABSTRACT

In future energy markets, traditional thermal power plants are expected to cycle more to adapt their operation to the intermittent power generation of renewable energy sources. Gas turbine load ramps and stresses in thick-walled equipment of the steam cycle are arguably the main limitations in the flexible operation of natural gas combined cycles. This work proposes a control strategy based on model predictive control with stress monitoring to overcome both limitations and enhance the flexible operation of thermal power plants. The linear and nonlinear formulation of the problem included in the model predictive control strategy are described, and two different modelling approaches for the stresses in the high pressure drum and steam turbine rotor are presented. The results demonstrate that the proposed control strategy is capable of computing optimal control sequences without exceeding the maximum allowable stress in critical components and the ramp rates of the gas turbine. The comparison between the linear and nonlinear formulations shows the superior performance of linear model predictive control and suggests that the nonlinear formulation should only be used when the stress models can not be expressed as a linear system of equations.

1. Introduction

Atmospheric concentrations of greenhouse gases are increasing as a result of the anthropogenic emissions since the industrial revolution [1]. According to the Intergovernmental Panel on Climate Change (IPCC), the temperature increase with respect to pre-industrial levels must not exceed 1.5 °C to limit the consequences of global warming in natural and human ecosystems [2]. Thus, a major reduction of greenhouse emissions in all sectors is necessary to migate the effects of climate change [2].

The energy sector is the main contributor to the global CO_2 emissions owing to its reliance on fossil fuels [3]. Renewable energy sources have increased their contribution in recent years in an effort to reduce the greenhouse emissions in this sector [3]. In line with this trend, more capacity will be installed with the objective of reaching 40% power generation from renewable energy sources by 2050 [4]. Consequently, thermal power plants will likely need to compensate the intermittency of renewable power generation and partly balance the load in the grid [5–9].

Flexible operation of thermal power plants will require enhanced cycling capabilities and more frequent start-ups and shut-downs [10–12]. Natural gas combined cycles (NGCC) offer the fastest operation with higher performance and lower emissions than traditional coal-fired power plants [13]. Therefore, NGCCs are expected to increase

☆ The short version of the paper was presented at ICAE2019, Aug 12–15, Västerås, Sweden. This paper is a substantial extension of the short version of the conference paper.

* Corresponding author.
E-mail addresses: jairo.r.pazos@ntnu.no (J. Rúa), lars.nord@ntnu.no (L.O. Nord).

https://doi.org/10.1016/j.apenergy.2020.114820
Received 18 November 2019; Received in revised form 6 March 2020; Accepted 7 March 2020

Nomenclature

Latin Symbols

A	system of equations matrix –
a	responses coefficients –
B	system of equations vector–
b	manipulated variables coefficients–
C	specific heat capacity J/kg K
c	nonlinear constraints–
cv	validity function centre –
d	QP optimization weight vector–
E	Young's Modulus MPa
e	stochastic error –
f	nonlinear objective function –
h	convection coefficient W/m^{2}K
k	heat conduction coefficient W/m K
M	number of local models –
N	time horizon –
p	pressure bar
Q	QP optimization weight matrix–
r	radius m
T	temperature deviation from design K
t	time s
U	manipulated variable –
u	displacement m
$\dot{W}$	mechanical power generation MW
w	validity function width –
$\hat{y}$	predicted response –
y	response –
z	vector of optimiaztion variables –

Greek Symbols

α	thermal diffusivity m^2/s
α^*	thermal expansion coefficient 1/K
γ	current operation point –
κ	current measurement vector –
λ	objective function weights –
ω	rotational speed rad/s
ρ	density kg/m^3
σ	stress MPa
υ	Poisson's ratio –
ξ	validity function –

Subscripts

θ	tangential direction
n_U	number past manipulated variables
n_y	number past responses
0	initial conditions
dist	displacement formulation
drum	high-pressure drum
eff	effective von Mises stress
effl	linearised von Mises stress
eq	equality
i	inner radius
ineq	inequality
int	integral formulation
m	metal
o	outer radius
r	radial direction
RH	reheated steam
SH	superheated steam
turb	first-stage steam turbine rotor
wall	wall of the equipment
z	longitudinal direction

Superscripts

high	higher bound
low	lower bound

their share in future energy markets [10].

Gas turbine load ramps and stresses in thick-walled components of the steam cycle are arguably the main limitations during the dynamic operation of NGCCs [14]. Fast load ramps may lead to combustion issues in the gas turbine, whilst excessive stress levels generate creep and fatigue in the walls of the equipment and reduce their expected operational lifetime. The maximum gas turbine load ramps are determined by the manufacturer and depend exclusively on the gas turbine model. In contrast, the stresses arising on the walls of the power plant equipment depend mainly on temperature gradients, inner and outer pressures, and centrifugal forces. These stresses can be limited by an adequate control strategy [15].

Monitoring the stress development on thick-walled components (e.g. high pressure steam turbine rotor and high pressure drum) is fundamental to enhance the flexible operation of thermal power plants and ensure their integrity [16–20]. Kim et al. [16] and Taler et al. [19,20] demonstrated how the adequate control of temperature and mass flow rates can limit the stress in a steam drum, whereas Can Gülen and Kim [18] showed the stress development in the high pressure drum and rotor of a combined cycle during the start-up sequence, pointing out the critical stresses that arise in this equipment. Alobaid et al. [17] proved that the start-up time can be reduced with adequate control strategies using PID controllers. As a result, larger temperature gradients and pressure differences built up in the equipment, leading to stresses that could damage these components. Stress monitoring was recommended to ensure that the proposed control did not exceed the limits of the material but was not included in their analysis.

Traditional PID control is not suitable for flexible operation of thermal power plants with stress prediction and monitoring as it is not possible to impose constraints on the controlled variables. Dynamic optimisation is a more advanced control approach where the control sequence is the result of an optimisation problem [21]. Therefore, the stress development can be computed simultaneously with the control actions where constraints may be imposed. As a result, optimal start-up sequences and load gradients that do not exceed the stress limits can be obtained with this approach [22–24].

Model predictive control (MPC) is a control methodology based on the periodic solution of a dynamic problem and the update of the optimal control actions. MPC predicts the performance of the power plant and selects the best control action based on the current state of the system. This control strategy can adjust the operation of the power plant to disturbances and demand changes by solving a dynamic optimisation problem periodically. In thermal power plants, MPC leads to better temperature, pressure and level control than traditional PID controllers or control strategies based on single dynamic problems [25–29]. In addition, Sindareh et al. [30] demonstrated the MPC capacity to control the temperature gradient in the steam turbine rotor and reduce its deterioration. However, the application of this control strategy is limited since deterioration depends on the stresses and not on the temperature gradient.

The first control methodology that included stress and load ramp limitation in the MPC control strategy of an NGCC was proposed by Rúa et al. [15]. Linear MPC was utilized for temperature control in the power plant and limit the stresses in the high pressure drum and the

high pressure steam turbine rotor. The results demonstrated that the proposed methodology was capable of computing the optimal control actions without exceeding the maximum allowable stresses.

This work complements and expands the previous work by proposing a novel stress modelling for both high pressure drum and rotor, and formulating the problem linearly and nonlinearly. Since thermal power plants are highly integrated by equipment with complex and different geometries, stress modelling may lead to nonlinear systems where linearisation is not accurate. Therefore, linear MPC is not suitable and nonlinear formulations of the optimal control problem with stress monitoring are necessary to ensure a safe yet efficient operation of thermal power plants. The two formulations proposed in this study ensure that this methodology can be applied to all control problems and any stress model can be embedded in the control strategy. This enhances the applicability range of the proposed methodology, as stress modelling of difficult geometries can be included in a nonlinear MPC for their application in control. Section 2 describes the dynamic model of the case study power plant, the simplified models implemented in the MPC, and the stress models of the drum and rotor. The control strategy and its mathematical formulation are described in Section 3. A comparison between the computational performance of the linear and nonlinear MPC formulations is presented in Section 4 with a case study that demonstrates the capability of the proposed control methodology to limit the stress development in the NGCC. Section 5 summarizes the main findings of this study.

2. Power plant and stress modelling

This work utilizes several models of different complexity to describe the stress in the equipment, predict the power plant performance and simulate the MPC application in a modern NGCC. This section describes the dynamic high-fidelity model utilized to replicate the transient behaviour of a thermal power plant, the simplified models implemented in the MPC to estimate the future thermodynamic state of the power plant at specific locations, and the stress models that are also embedded in the MPC optimisation problem to avoid that the limits of the materials are exceeded.

2.1. Natural gas combined cycle dynamic model

Natural gas combined cycles with triple pressure steam cycles and reheating are the thermal power plants that offer the highest efficiency with the lowest emissions [14,31]. A dynamic high-fidelity model of a modern NGCC is utilized in this work to study the performance of the proposed MPC methodology on this type of power plants and replicate the behaviour of a real NGCC. Fig. 1 represents the configuration of the NGCC considered in this work. The steady state design was carried out in GT PRO [32] because it provides detailed information of the geometry of the equipment that is necessary for the dynamic model, e.g. the dimensions, materials and number of units of the different components.

The dynamic high-fidelity model of the NGCC was constructed using the Thermal Power library [33] in the software Dymola [34], which is based on the Modelica language [35]. This dynamic model is based on first principle equations for fluid flow, includes thermodynamic properties for the different fluids in the NGCC, and switches among different pressure and heat transfer correlations depending on the fluid state. Pump modelling is based on maps of performance from operation data, whilst the steam turbine model is defined by Stodola cone law. Since the gas turbine transient performance is orders of magnitude faster than the steam cycle, a quasi-steady state model was used to provide the mechanical power output, and the temperature and pressure of the exhaust gas. Software to software validation at design and off-design operation demonstrated the accuracy and reliability of the dynamic NGCC model. A thorough description of the modelling approach and validation of the NGCC model is presented in the work by Montañés et al. [36].

2.2. Simplified models of the natural gas combined cycle

Good control strategies must be capable of anticipating the dominant dynamics of the system to maintain a stable and efficient operation. Therefore, the dominant dynamics of the system dictate the frequency of the control actions. For control strategies based on MPC, computational speed is the main limitation. As model predictive control

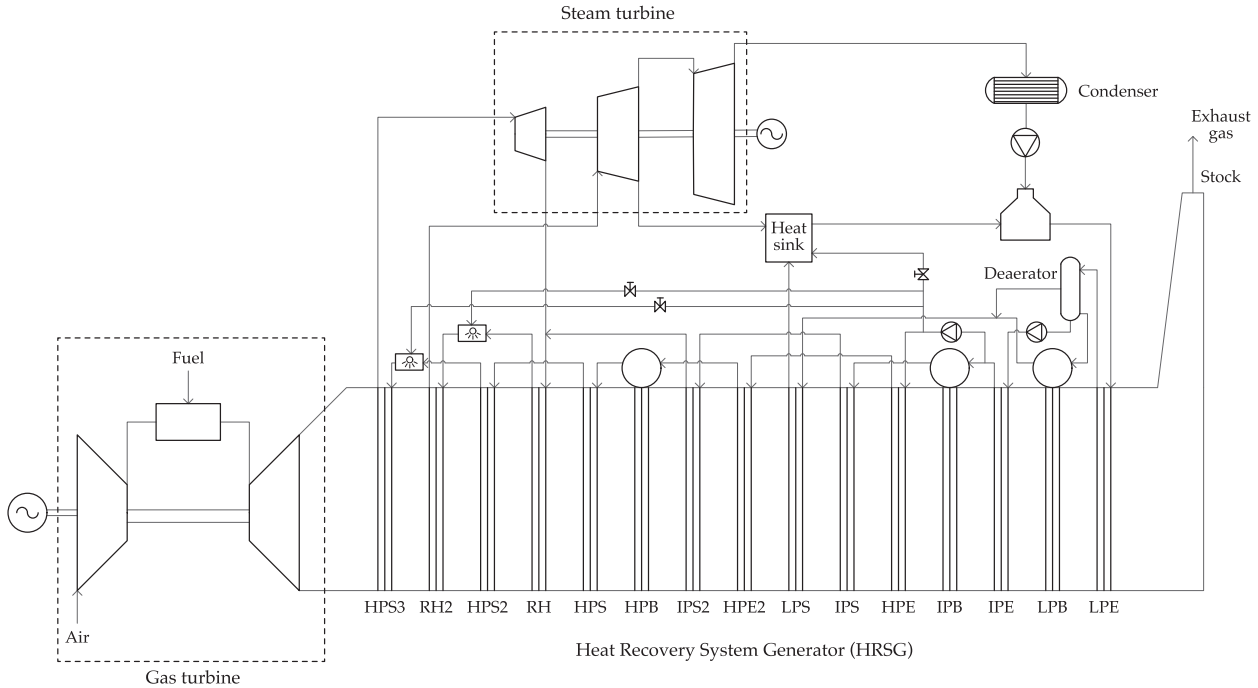

Fig. 1. Process model of the natural gas combined cycle. The nomenclature in the HRSG is as follows. E: Economizer, B: Boiler, S: Superheater, R: Reheater P: Pressure, L: Low, I: Intermediate, H: High.

relies on the periodic solution of a dynamic optimisation, fast dominant dynamics require fast online optimisation and control. The dominant dynamics of modern NGCCs with 600 MW power output occur approximately in 300 s. Thus, the control actions should be imposed every 15–30 s to anticipate and meet the transient operation of the power plant. A sampling time of 30 s was found as a reasonable trade-off between controllability and computational time for the dynamic optimisation. The dynamic high-fidelity model cannot be used in the MPC strategy because it would lead to excessively high optimisation times for online operation with current computational power, owing to its complexity. Simplified models that predict the behaviour of key thermodynamic variables in the power plant must be used instead.

Autoregressive models with exogenous variables (ARX) are linear data-based models that can predict the dynamic performance of a system. These models are suitable for dynamic optimisation because of their simplicity and accuracy within the training data range [37]. System identification was the approach followed to develop the ARX models and combined them in a local model network that can predict nonlinear behaviour with a set of linear local models [25,38].

The data to train and test the ARX models was obtained by superimposing random gaussian signals (RGS) in the controllers of the dynamic high-fidelity model in closed-loop [39–42]. Different sets of data were generated for each operation regime and variable, and least squares were used to fit the training data to the general ARX model structure:

$$y(t) + a_1\, y(t-1) + \cdots + a_{n_y}\, y(t-n_y) = b_1\, U(t-1) + \cdots + b_{n_U}\, U(t-n_U) + e(t) \quad (1)$$

where n_y and n_U denote the order of the model, y represents the predicted variable, U are independent variables, and $e(t)$ is a white-noise term that enters in the regression as prediction error.

The operation regime defines the prediction range of each linear local model. Several local models are necessary to cover the operation range of a variable in the high-fidelity model, which normally exhibits nonlinear behaviour. A local model network combines the local models and interpolates their prediction according to the operating point of the NGCC. The interpolation is achieved by associating to each local model a validity function, which weights the contribution of the local models to the final output depending on the operating point. This approach ensures that neighbouring local models contribute more to the final output than local models for distant operation regimes [25,38]. Fig. 2 represents the structure of a generic local model network.

A Gaussian validity function was selected to interpolate the different local models of each variable [38]:

$$\xi_i(\gamma) = \frac{exp\left(-\frac{1}{2}\,[(\gamma - cv_i)/w_i]^2\right)}{\sum_{k=1}^{M} exp\left(-\frac{1}{2}\,[(\gamma - cv_i)/w_i]^2\right)} \quad (2)$$

where cv_i and w_i are, respectively, the centres and widths of the local Gaussian interpolation functions.

The final output of the local model network is a combination of all local outputs:

$$\hat{y}(t) = \sum_{i=1}^{M} \hat{y}_i(\kappa)\, \xi_i(\gamma) \quad (3)$$

where M is the number of local models, $\hat{y}_i(\kappa)$ represents the outputs of the local ARX models under the conditions defined by the inputs κ, ξ is the local validity function associated to each ARX model, and γ is the parameter defining the current operating point.

In this work, the variable defining the operating point (γ) was the gas turbine load and 5 equidistant local models in the range 100–60% were defined for each of the predicted variables. The mechanical net power generation of the NGCC, and the superheated and reheated steam temperatures were the predicted variables using local model networks. The parameters of the Gaussian validity function were selected by a nonlinear optimisation [25,38]. A screening of different model orders, n_y and n_U, defined the ARX model structure that better predicted the testing data for 1 and 20 steps-ahead prediction (Fig. 3).

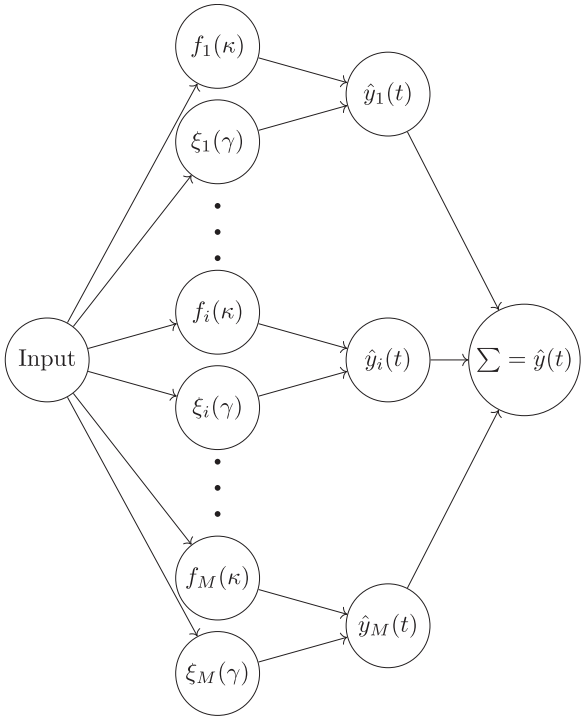

Fig. 2. Structure of a generic local model network.

In addition, simplified models for the saturation temperature and pressure in the steam drum and the inlet pressure in the steam turbine were also developed. Linear polynomials as in Eq. (4) are suitable models for these variables as they can be directly related to the gas turbine load.

$$\hat{y}(t) = a_0 + b_1\, U(t-1) \quad (4)$$

Table 1 summarizes the structure and main validation results of the models implemented in the MPC strategy. From these results, accurate predictions can be expected throughout the time horizon in the dynamic optimisation.

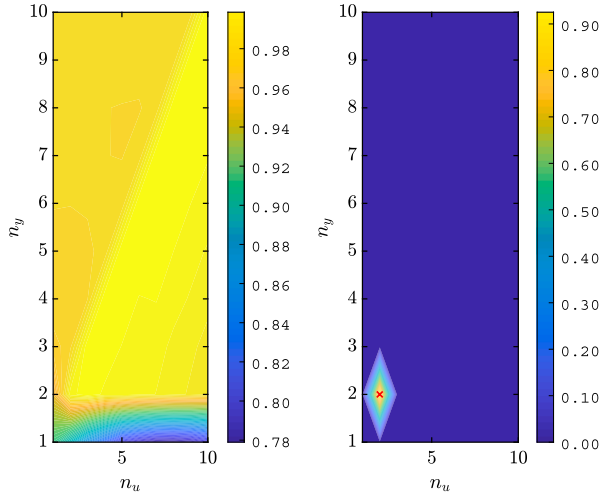

Fig. 3. Screening of different orders for the simplified model of the superheated steam temperature. One step-ahead prediction in the left and 20 step-ahead prediction in the right.

Table 1
Structure and 20 step-ahead validation results of the simplified models.

Variable	Model	Order	R^2_{20}
$\dot{W}_{net}$	LMN	(1,1)	99.95%
T_{SH}	LMN	(2,2)	76.97%
T_{RH}	LMN	(2,2)	92.82%
T_{drum}	Polynomial		86.16%
p_{drum}	Polynomial		85.22%
p_{turb}	Polynomial		86.62%

2.3. Stress modelling

Equipment with thick walls normally suffers the largest stresses in the thermal power plant. The main causes of these stresses are the large temperature gradients along the walls, the centrifugal forces due to rotation, and the high pressures this equipment must withstand. The high pressure drum and the rotor disk in the first stage of the high pressure steam turbine are arguably the most sensitive equipment in an NGCC [14,18]. Therefore, it is critical to ensure that the maximum allowable stress in those components is not exceeded during transient operation.

Thermal stresses depend on the temperature gradients along the wall. Thus, the temperature distribution is necessary to compute the thermal component of the stress in both drum and rotor. The temperature was assumed to vary exclusively in radial direction, reducing the modelling of the temperature distribution to the one-dimensional heat equation:

$$\frac{1}{r}\frac{\partial}{\partial r}\left(r\frac{\partial T}{\partial r}\right) = \frac{1}{\alpha}\frac{\partial T}{\partial t} \tag{5}$$

where T refers to the temperature difference respect to the equipment design temperature, r is a generic radius, and α is the thermal diffusivity of the material.

An implicit Crank-Nicolson scheme was used to discretize Eq. (5) and compute the temperature distribution along the walls. Different boundary conditions apply to the steam drum and rotor disk. The implementation of these boundary conditions and the mathematical development to express Eq. (5) as a linear system of equations are detailed in the work by Rúa et al. [15].

Stress modelling in the rotor and drum assumes plane strain and plane stress, respectively. These assumptions are valid because the longitudinal length of the steam drum is notably larger than in the other two directions, and negligible in the case of the rotor disk [43].

This work proposes and compares two different physical approaches to model the thermal and mechanical stresses with the considered assumptions. Both methods rely on the constitutive equations that relate the stress and strain, the strain-displacement relations, and the radial equilibrium equation. In addition, the mechanical stress due to the centrifugal force originated by the rotation enters as a body force, and the mechanical stress due to pressure appears as a boundary condition. The first modelling approach combines these equations to express the stress components in terms of the radial temperature distribution and the displacement. These expressions and a thorough description of the process to transform them in a linear system of equations can be found in the work by Rúa et al. and the supplementary material included therein [15].

In the second modelling approach, the ordinary differential equation obtained for the displacement is solved analytically. Thus, the displacement is not a computed variable and the stress components only depend on the temperature distribution, the rotational speed and the pressure. The stress components of the drum and rotor are defined in Eqs. (6) and (7), respectively.

$$\sigma_r = \left(1 - \frac{r_i^2}{r^2}\right)\frac{E\,\alpha}{(1+\upsilon)(1-2\upsilon)}\int_{r_i}^{r_o} rT\,\mathrm{d}r - \frac{E\,\alpha}{(1-\upsilon)}\int_{r_i}^{r} rT\,\mathrm{d}r + r + \left[\frac{r_o^2 r_i^2}{(r_o^2 - r_i^2)r^2} - \frac{r_o^2}{(r_o^2 - r_i^2)}\right](p_o - p_i) - p_i \tag{6a}$$

$$\sigma_\theta = \left(1 + \frac{r_i^2}{r^2}\right)\frac{E\,\alpha}{(1-\upsilon)(r_o^2 - r_i^2)}\int_{r_i}^{r_o} rT\,\mathrm{d}r + \frac{E\,\alpha}{1-\upsilon}\left(\frac{1}{r^2}\int_{r_i}^{r} rT\,\mathrm{d}r - T\right) + \left[\frac{r_o^2 r_i^2}{(r_o^2 - r_i^2)r^2} + \frac{r_o^2}{(r_o^2 - r_i^2)}\right](p_i - p_o) - p_i \tag{6b}$$

$$\sigma_z = \frac{2\upsilon E\,\alpha}{(r_o^2 - r_i^2)(1-\upsilon)}\int_{r_i}^{r_o} rT\,\mathrm{d}r - \frac{E\,\alpha}{1-\upsilon}T + p_i\left(\frac{2\upsilon r_o^2}{r_o^2 - r_i^2} - 2\upsilon\right) - p_o\frac{2\upsilon r_o^2}{r_o^2 - r_i^2} \tag{6c}$$

$$\sigma_r = \left[1 + \upsilon + \frac{(1-\upsilon)r_i^2}{r^2}\right]\frac{r_o^2}{(1+\upsilon)r_o^2 + (1-\upsilon)r_i^2}\left(\frac{E\,\alpha}{r_o^2}\int_{r_i}^{r_o} rT\,\mathrm{d}r - p_o\right) - \frac{E\,\alpha}{r^2}\int_{r_i}^{r} rT\,\mathrm{d}r + \frac{\rho\,\omega^2 r_o^2(1+\upsilon)}{8[(1+\upsilon)r_o^2 + (1-\upsilon)r_i^2]}[r_o^2(3+\upsilon) - r_i^2(1+\upsilon)] + \frac{\rho\,\omega^2}{8}[(1+\upsilon)r_i^2 - (3+\upsilon)r^2] + \frac{\rho\,\omega^2 r_o^2 r_i^2(1-\upsilon)}{8r^2[(1+\upsilon)r_o^2 + (1-\upsilon)r_i^2]}[r_o^2(3+\upsilon) - r_i^2(1+\upsilon)] \tag{7a}$$

$$\sigma_\theta = \left[1 + \upsilon - \frac{(1-\upsilon)r_i^2}{r^2}\right]\frac{r_o^2}{(1+\upsilon)r_o^2 + (1-\upsilon)r_i^2}\left(\frac{E\,\alpha}{r_o^2}\int_{r_i}^{r_o} rT\,\mathrm{d}r - p_o\right) + E\,\alpha\left(\frac{1}{r^2}\int_{r_i}^{r_o} rT\,\mathrm{d}r - T\right) + \frac{\rho\,\omega^2 r_o^2(1+\upsilon)}{8[(1+\upsilon)r_o^2 + (1-\upsilon)r_i^2]}[r_o^2(3+\upsilon) - r_i^2(1+\upsilon)] + \frac{\rho\,\omega^2}{8}[(1+\upsilon)r_i^2 - (1+3\upsilon)r^2] + \frac{\rho\,\omega^2 r_o^2 r_i^2(1-\upsilon)}{8r^2[(1+\upsilon)r_o^2 + (1-\upsilon)r_i^2]}[r_i^2(1+\upsilon) - r_o^2(3+\upsilon)] \tag{7b}$$

Table 2
Validation boundary conditions.

Component	Thermal Boundary Conditions				Mechanical Boundary Conditions		Rotation
	$T_{initial}$	Ramp	h_i	h_o	r_i	r_o	
Drum	340 [°C]	± 20	20000 [W/m²K]	0.065 [W/m²°C]	p = 150 [bar]	p = 1 [bar]	–
Rotor	590 [°C]	± 10	-	20000 [W/m²°C]	u = 0 [m]	p = 140 [bar]	3000 [rpm]

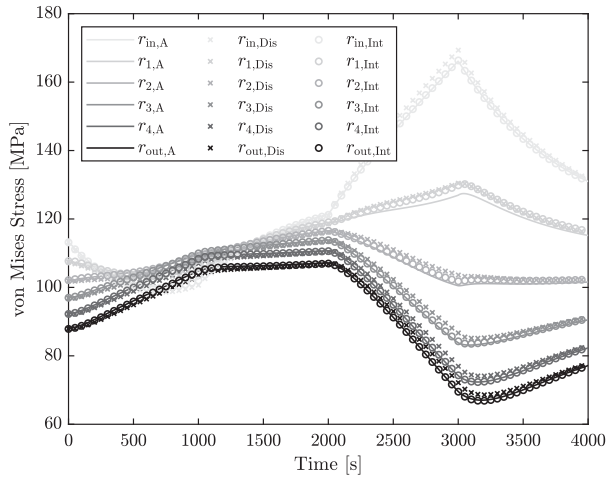

(a) von Mises equivalent stress along six equidistant radii of the drum.

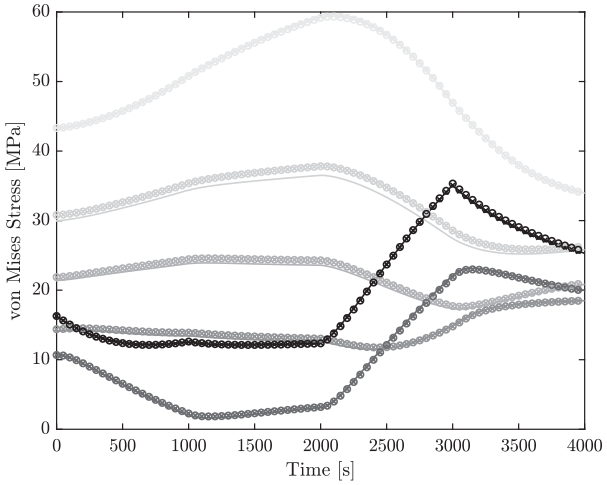

(b) von Mises equivalent stress along six equidistant radii of the rotor disk.

Fig. 4. Validation results of the stress models for the two proposed approaches. *A* refers to the results obtained in ANSYS, Dis refers to the modelling approach based on computing the displacement, and Int to the approach based on applying the trapezoidal rule to the integrals in Eqs. (6) and (7).

Linear MPC requires that the models implemented in the dynamic optimisation problem are linear. Therefore, the trapezoidal rule was applied to Eqs. (6) and (7) so they can be expressed as a linear system of equations.

The von Mises equivalent, or effective, stress defined in Eq. (8) is a scalar measure of the overall effective stress, as it is combination of the different stress components. Therefore, a constraint is imposed on the von Mises equivalent stress in the optimisation problem to ensure that the maximum effective stress is not exceeded. A linearisation of the von Mises stress, defined in Eq. (9), is used in the linear MPC formulation.

$$\sigma_{\text{eff}}^2 = \sigma_r^2 + \sigma_\theta^2 + \sigma_z^2 - (\sigma_r\sigma_\theta + \sigma_\theta\sigma_z + \sigma_z\sigma_r) \tag{8}$$

$$\sigma_{\text{effl}}^2 = \sigma_{\text{effl},0}^2 + \nabla\sigma_{\text{effl},0}^2\Delta\sigma + \mathcal{O}(\Delta x^2) \tag{9}$$

Model validation of the two approaches considered in this work was carried out with the specialized software ANSYS [44]. Table 2 summarizes the boundary conditions imposed to the models during the validation procedure. Structural steel was the material assumed for both drum and rotor as it has well-known properties. A comparison between the accuracy of both approaches is presented in Fig. 4.

3. Control methodology with stress monitoring

Natural gas combined cycles exhibit two different dominant dynamics. Gas turbines have negligible dynamics and can change their operation point within a few seconds. In contrast, the large metal mass of the heat recovery steam generator (HRSG) in the steam cycle limits its transient operation. The heat capacity of this bulk component leads to dominant dynamics between 10 and 20 min, depending on the size of the NGCC. Power generation is however not limited by the slow dynamics of the steam cycle as gas turbines can over- and under-shoot to compensate its slow response, leading to tight power generation control [15].

As power control relies mainly on the gas turbine, the steam cycle normally operates in sliding pressure mode due to the higher efficiency of this strategy [31,45]. This type of operation keeps the admission valves of the steam turbine close to fully open to maintain the volume flow constant whilst the pressure of the steam cycle can vary freely. Throttling at the inlet of the steam turbine is hence avoided until about 50% load, where it becomes necessary for the HRSG operation [31].

The control of the steam cycle between 100% and 50% load reduces to limiting the steam temperature at the inlet of the steam turbine, and control of the fluid inventory and low pressure in the cycle. Both traditional PID controllers and more advanced MPC strategies can be used to ensure the adequate operation of the steam cycle [27–29,46]. In this work, inventory and low pressure control in the steam cycle was carried out by PID controllers [36], whereas MPC was implemented to control the power generation of the NGCC and limit the superheated and reheated steam temperature at the inlet of the steam turbine. Attemperator valves regulate the temperature of the steam at the inlet of the steam turbine, and the gas turbine load controls the power generation of the NGCC. In addition, stress monitoring and control was included in the MPC strategy to ensure that the maximum allowable stress in the high pressure drum and rotor disk were not exceeded during the transient operation of the NGCC. Stress levels close to the limit of the material impose restrictions on the load change of the gas turbine and may slow down the NGCC.

In some cases, stresses in different equipment might only be expressed as nonlinear models; whereas linear formulations are exclusively used in other applications. Therefore, both linear and nonlinear formulations of the dynamic optimisation problem in the MPC strategy are presented so any stress model can be implemented. This expands the applicability range of the proposed control methodology to any type of control problem with stress monitoring.

3.1. Linear MPC formulation

Linear MPC solves a dynamic quadratic programming (QP) problem every sampling time. The mathematical formulation of this optimisation problem is:

$$\min_{z\in\mathbb{R}^n} f(z) = \frac{1}{2}z^T Q z + d z \tag{10a}$$

subject to

$$A_{\text{eq}}\, z = B_{\text{eq}} \tag{10b}$$

$$A_{\text{ineq}}\, z \leqslant B_{\text{ineq}} \tag{10c}$$

$$z^{\text{low}} \leqslant z \leqslant z^{\text{high}} \tag{10d}$$

with

$$Q \succcurlyeq 0 \tag{10e}$$

Vector z represents the optimisation variables of the optimisation problem. These are the manipulated variables defining the control

actions (U in Eqs. (1) and (4)), the responses $\hat{y}$ associated to them, and the temperature distribution, stress components and linearised equivalent stress in the wall of the drum and rotor disk. Eq. (10d) includes the lower and upper bounds of these optimisation variables, including the maximum allowable stress that the material of the equipment can withstand.

The simplified models and the stress linear system of equations developed in Section 2 enter in the optimisation problem as linear equality constraints in Eq. (10b). This ensures that the solution respects the stress physics and the thermodynamic behaviour of the NGCC. Similarly, the limitation in the maximum load ramp of the gas turbine is implemented in Eq. (10c).

During the dynamic optimisation, the degrees of freedom, i.e. the manipulated variables of the system, are continuously modified until a set of optimisation variables z that minimizes the objective function defined by Eq. (10a) is obtained. Minimizing the difference between power generation and demand, and the deviation of the superheated and reheated steam temperature from their set-points were the objectives in this work. Q and d are a weight matrix and vector, respectively. The description of the matrices and vectors in Eq. (10) with the stress modelling approach including the displacement can be found in the work by Rúa et al. [15].

3.2. Nonlinear MPC formulation

The nonlinear programming (NLP) problem used in the nonlinear MPC strategy is mathematically formulated as:

$$\min_{z \in \mathbb{R}^n} f(z) \tag{11a}$$

subject to

$$c_{\text{eq}}(z) = 0 \tag{11b}$$

$$c_{\text{ineq}}(z) \leqslant 0 \tag{11c}$$

$$A_{\text{eq}}\, z = B_{\text{eq}} \tag{11d}$$

$$A_{\text{ineq}}\, z \leqslant B_{\text{ineq}} \tag{11e}$$

$$z^{\text{low}} \leqslant z \leqslant z^{\text{high}} \tag{11f}$$

where z represents the vector of optimisation variables with lower and upper bounds defined in Eq. (11f), c_{eq} and c_{ineq} are, respectively, nonlinear equality and inequality constraints, and Eqs. (11b) and (11c) are their linear counterparts. The objective function $f(z)$ defined in Eq. (11a) can be any linear or nonlinear function.

This mathematical formulation adds modelling flexibility as the simplified and stress models can enter the dynamic optimisation in Eqs. (11b) or (11d), and ensures that the physics of the system and the stresses are always met regardless of the linearity of the models. Eqs. (11c) and (11e) provide the same benefits with the inequality constraints.

The same simplified models and linear system of equations describing the stresses were implemented in the nonlinear optimisation problem to compare the linear and nonlinear MPC formulation and the two proposed approaches to model the stresses in the drum and rotor disk. Therefore, the simplified models enter as a linear equality constraint in Eq. (11d) and the constraint in the gas turbine load ramp as a linear inequality constraint in Eq. (11e). In the NLP problem, the von Mises equivalent stress defined in Eq. (8) is used instead of the linearized version defined in Eq. (9) and implemented in the QP problem. This model represents a nonlinear constraint in the nonlinear dynamic optimisation problem.

Albeit the only difference between the linear and nonlinear MPC formulation is the utilization of a different equation to calculate the equivalent von Mises stress, the optimisation problem changes notably. In the QP optimisation problem, the linearized von Mises equivalent stress is expressed together with the models of the temperature distribution, displacement (if the first modelling approach is considered) and stress components in a linear system of equations. All these variables are hence optimisation variables since this system of equations is implemented in the optimisation problem as a linear equality constraint. In contrast, the only optimisation variable in the NLP problem is the von Mises equivalent stress. As the nonlinear inequality constraint in Eqs. (11c) does not require an entire system of equations, only the variables of interest may be defined as optimisation variables.

Therefore, the QP optimisation problem in the linear MPC formulation has more optimisation variables than the NLP problem. However, checking whether the nonlinear constraints are satisfied requires more evaluations of the stress models than in the QP problem. Section 4 illustrates which of these two optimisation problems, and thus MPC formulations, leads to better computational performance.

4. Results and discussion

Linear and nonlinear MPC with stress control differ on the number of optimisation variables and how evaluate the stress models. The computational performance of the QP and NLP optimisation problems is crucial for the utilization of MPC as control strategy due to the limited time to carry out the dynamic online optimisation. Thus, the computational time required by both formulations with the two stress modelling approaches proposed in this work was compared for a single optimisation.

The proposed control methodology was also tested in a case study where tight limitations on the maximum allowable stress in the drum were included. This reduced the operational margin of the NGCC and forced the MPC controller to adequate the control actions imposed on the manipulated variables. These scenarios are specially relevant in power markets dominated by the large deployment of renewable energy sources, where thermal power plants will most likely balance the grid, leading to more frequent start-ups, shut-downs and faster load ramps that will narrow the operational limits.

4.1. Computational time analysis

A dynamic optimisation with the simplified models defined in Section 2 and a time horizon of 30 sampling times was the test case used to compare the computational time of the QP and NLP optimisation problem. In addition, the stress models defined with the two proposed approaches were included in order to compare their effect on the computational cost. Table 3 summarizes the computational time for each formulation and stress modelling approach relative to the fastest optimisation.

Quadratic programming shows superior computational performance independently of the stress modelling that is implemented. This demonstrates that, albeit having less optimisation variables, the evaluation of the objective function gradients and the stress models as nonlinear constraints suppose big penalties on the computational cost that lead to longer computational times. The gradients of the objective function in the QP optimisation problem are computed analytically, whilst in the NLP case the gradients are calculated numerically by finite differences. This leads to an increase of performance of the linear formulation. As a result, linear MPC can carry out more optimisations in a

Table 3
Relative computational time for the both MPC formulations and stress modelling approaches. Disp refers to the stress model based on the displacement calculation and Int to the integral stress model.

Formulation	Linear		Nonlinear	
Stress Model	Disp	Int	Disp	Int
Relative Time	1.88	1	41.02	27.19

given period of time, which allows to increase the time horizon during the optimisation, reduce the sampling time, or include more models in the constraints of the QP problem. These modifications would result in tighter and more frequent control actions that would improve performance of the power plant, and could expand the stress monitoring to other components that can also be critical in scenarios such start-ups and shut-downs.

The stress modelling approach does not have a strong effect on the computational time. The model based on the integral definitions of the stress components leads to slightly faster results than those obtained from the model additionally computing the displacement. This behaviour may be explained by the reduction of optimisation variables in the integral-based approach as the displacement is not computed. However, this approach leads to denser matrices in the linear system of equations than those obtained with the displacement-based approach, which are more sparse. The number of spatial discretizations along the wall of the components is also different for each of these two modelling approaches. Since the matrices obtained from the integral stress equations are denser due to the extra analytical development integrating the ordinary differential equations, they have more information and hence less spatial discretizations are needed. In contrast, the sparsity of the matrices obtained from the displacement-based models require more discretizations to capture the physics on the wall of the drum and rotor. Therefore, the computational time of the dynamic optimisation is affected by the number of spatial discrezations. Because of their similar accuracy (see Fig. 4), the relative small difference in computational time, and the difference in space discretizations needed by each model, both stress modelling approaches are suitable for utilization in MPC strategies.

4.2. Flexible operation with stress limitation

A load step change of 25% was the selected scenario to test the control methodology proposed in this work. This simulates a reduction in the power demand of 165 MW that the NGCC needs to compensate by decreasing its power generation as fast as possible without exceeding the maximum allowable stress in the steam drum and rotor disk, and limiting the maximum temperature at the inlet of the steam turbine.

These operational limitations were implemented in the optimisation problem of the MPC strategy as the objective function and constraints (see Section 3). The weights in the matrix Q and vector d of the objective function used in this simulation were $\lambda_{y_1} = 1$ for the power generation, and $\lambda_{y_2} = \lambda_{y_3} = 10$ for the temperature deviations from the set-point. The penalties in the manipulated variables, i.e. gas turbine load and attemperator valves, were $\lambda_{U_1} = \lambda_{U_2} = \lambda_{U_3} = 2$. The time horizon was 30 to guarantee that the system dynamics were captured, and a sampling time of 30 ensured that the control actions were implemented with enough frequency to anticipate the dominant dynamics of the system. For the stress models of the high pressure drum and rotor disk, 200 and 50 spatial discretizations were selected, respectively, whilst 3 time discretizations per sampling time were used.

Table 4 summarizes the physical and mechanical properties considered for the drum and rotor disk [47]. Since the maximum allowable stress presented in Table 4 was not reached with a realistic value during the considered scenario, a reduced value of the yield stress of 125 MPa was used to demonstrate the capability of the control methodology to predict the stress and adapt the operation of the power plant. Both simulations limited the maximum gas turbine load ramp to 15% per minute. Table 5 includes the lower and upper bounds of the optimisation variables.

Stress constraints may notably affect the operation of thermal power plants. Fig. 5 shows how the maximum allowable stress in the high pressure steam drum slows down the reduction in mechanical power generation. Lower limits in the equivalent stress of the equipment reduce the operating region of the NGCC. The MPC strategy is still able to compute optimal control sequences but the power ramp down is slower than in the case with looser constraints. Fig. 6 presents the two optimal load profiles of the gas turbine that the MPC computed for the two scenarios with different stress limits on the steam drum. Albeit the gas turbine load varies identically in the first seconds, the stress development due to the transient operation of the NGCC forces the MPC strategy to reduce the rate of change of the gas turbine load and hence the reduction of power generation.

The stress in three equidistant radii of the wall of the steam drum and rotor disk during the change of operation of the NGCC is represented in Figs. 7 and 8, respectively. Lower stress limits change the stress development profiles in the wall of this equipment because of the different transient operation determined by the MPC strategy. Fig. 7 illustrates how the dynamic optimisation problem in the MPC strategy reaches the maximum allowable stress constraint in the drum, which is active during 300–400 s, thus inhibiting larger changes in the gas turbine load and slowing the transient operation of the NGCC. The stress profile where the maximum allowable stress is 190 MPa (black lines) demonstrates that higher limits on the material allow larger stress developments and enhance the flexible operation of the NGCC. Therefore, the power plant can ramp down faster and meet the power demand in less than 300 s by under-shooting the gas turbine to compensate the slowness of the steam cycle.

Both the stress estimated during the optimisation in the MPC strategy and the exact stress computed with the true temperature and pressure profiles are compared in Figs. 7 and 8. The stress prediction during the dynamic optimisation captures the tendency of the stress development, as the different between the true stress and this prediction is small. However, the stress models over-predict the effective stress when the transient operation starts, specially in the steam drum. This behaviour may be explained by the lack of detailed data of the temperature distribution in the high-fidelity NGCC model, which forces the MPC controller to estimate the initial temperature along the walls of the equipment and provide this information to the dynamic optimisation problem. Stress prediction during the control of the NGCC operation would improve if the actual temperature distribution was provided by the detailed dynamic model of the NGCC.

Temperature control is also affected by the limitations imposed by the maximum allowable stress. Figs. 9 and 10 show the different temperature profiles obtained during the two test cases. Tighter stress limits lead to slower ramps in the gas turbine and more progressive changes in the steam cycle. Slower temperature variations are thus observed in the superheated and reheated steam. Consequently, tighter limits on the effective stress in the equipment of the NGCC ease the temperature control. Nevertheless, the proposed MPC strategy can rapidly limit the steam temperature variation without exceeding the temperature limitations in both test cases.

Table 4
Physical and mechanical properties of the materials considered for the drum and rotor disk.

Component	Material	ρ [kg/m^3]	C_m [J/kg K]	k_m [W/m K]	α^* [m^2/s]	α [1/K]	E [MPa]	υ[−−]	h_o [W/m^2 K]	h_i [W/m^2 K]	Yield stress [MPa]
Drum	SA-515 Grade 70	7850	434	47	1.3796e−05	1.36e−5	178000	0.3	5000	0.065	190
Rotor	X18CrMnMoNbVN12	7700	460	29	8.1875e−06	1.25e−5	127000	0.292	4000	–	69

Table 5
Lower and upper bounds of the optimisation variables.

LMN			Drum			Rotor		
Lower	Variable	Upper	Lower	Variable	Upper	Lower	Variable	Upper
400	$\dot{W}$	615.867	$-\infty$	T_{wall}	∞	$-\infty$	T_{wall}	∞
-10	T_{SH}	15	-0.001	u	0.001	-0.001	u	0.001
-10	T_{RH}	15	$-\infty$	σ_r	∞	$-\infty$	σ_r	∞
$-\infty$	p_{turb}	∞	$-\infty$	σ_θ	∞	$-\infty$	σ_θ	∞
$-\infty$	T_{drum}	∞	$-\infty$	σ_z	∞	0	σ_{eql}	69
$-\infty$	p_{drum}	∞	0	σ_{eql}	190/125			
60	U_1	100						
-0.01655	U_2	0.97345						
-0.06882	U_3	0.92188						

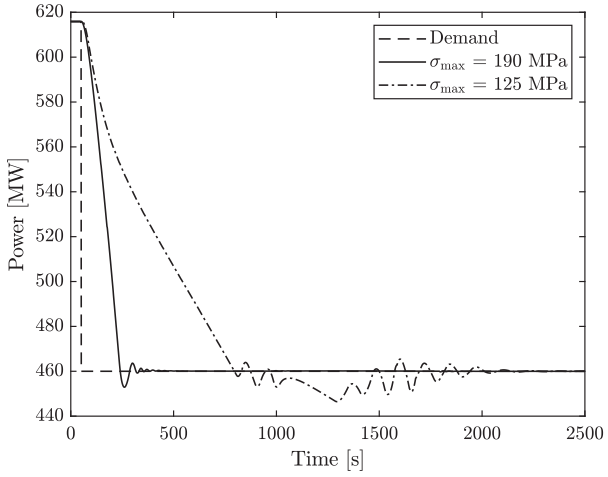

Fig. 5. Mechanical power generation with different stress constraints in the drum.

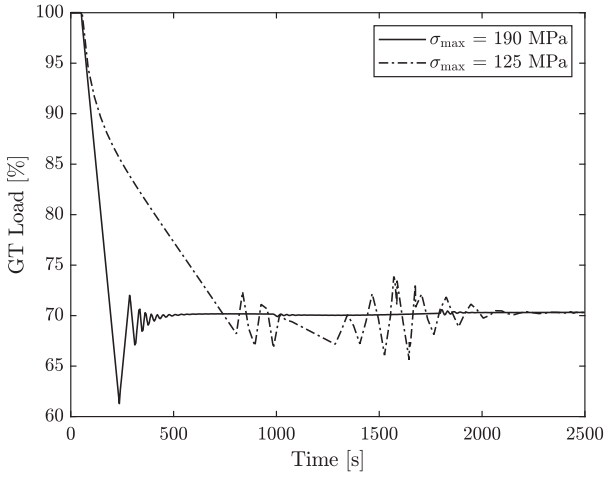

Fig. 6. Gas turbine load profile with different stress constraints in the drum.

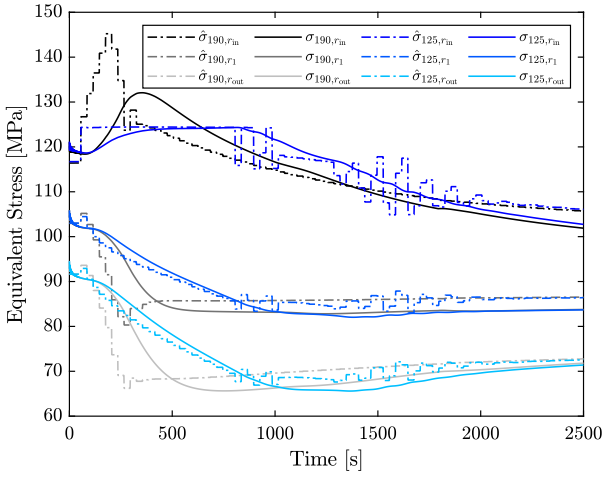

Fig. 7. Equivalent stress in the high pressure steam drum along three equidistant radii.

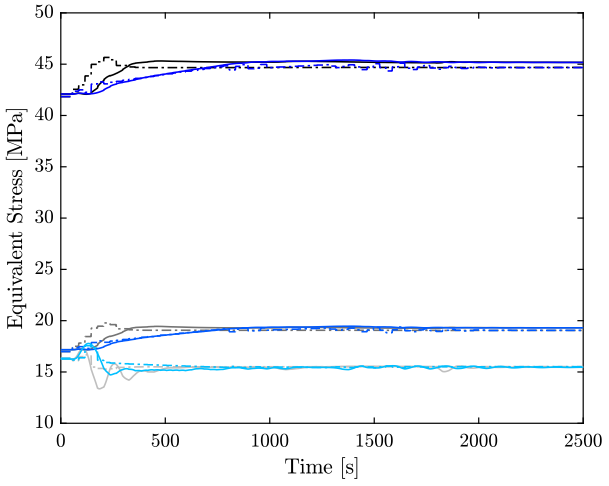

Fig. 8. Equivalent stress in the high pressure rotor disk along three equidistant radii.

5. Conclusions

Thermal power plants will need to ramp faster and more frequently to balance the intermittent power generation from renewable energy sources in the future energy sector. Gas turbine load ramps and thermal stresses limit the power generation rate. This work addresses both limitations by proposing a control strategy based on model predictive control with stress monitoring.

Two modelling approaches for the stresses in the walls of the high pressure steam drum and the rotor disk of the first stage of the steam turbine were proposed. Furthermore, both linear and nonlinear MPC formulations were described to cover all possible control problems and modelling approaches of the stresses in different equipment. Local model networks of simplified models were also developed to predict specific thermodynamic variables of the NGCC during the dynamic optimisation.

A comparison of the computational cost of the linear and nonlinear dynamic optimisation problems proved the superior performance of the linear MPC formulation. Nonlinear MPC requires more evaluations of

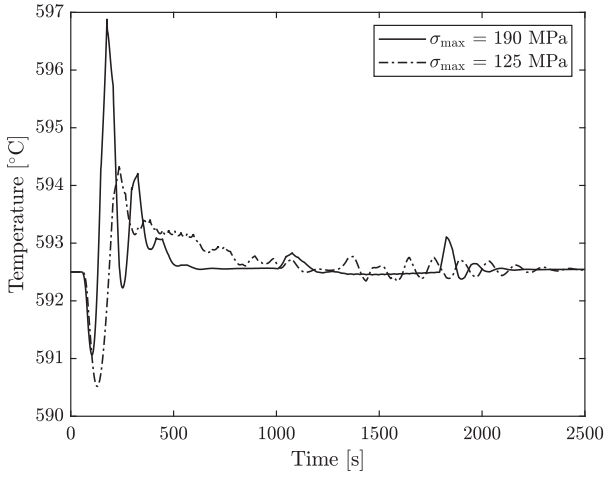

Fig. 9. Superheated steam temperature with different stress constraints in the drum.

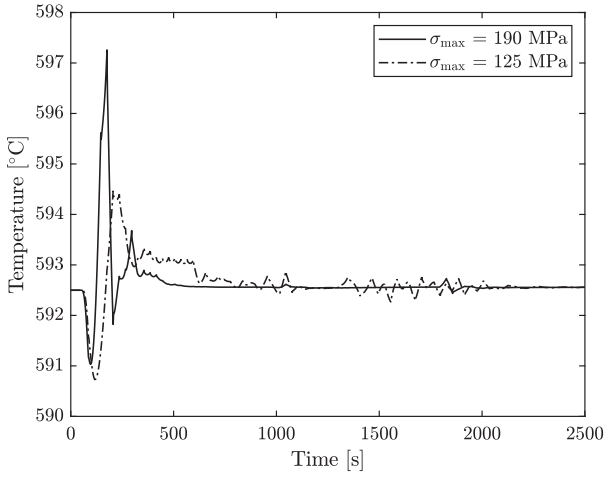

Fig. 10. Reheated steam temperature with different stress constraints in the drum.

the stress models than the linear formulation to compute numerically the gradients of the optimisation problem by finite differences, leading to longer computational times despite having less optimisation variables. Thus, linear MPC is more advantageous when is possible to employ linear models to predict the thermodynamic variables of the NGCC and the stress development in the walls of the selected equipment. It is possible to resort to nonlinear MPC when modelling of the stresses or simplified models cannot be carried out with linear formulations.

The two proposed modelling approaches to estimate the equivalent stress in the walls of the steam drum and rotor disk proved similar accuracy during their validation. Both stress models led to similar computational times during the dynamic optimisation. The difference showed in Table 3 is originated by the different spatial discretizations. Since these two modelling approaches lead to linear system of equations with different sparsity in the matrices, different spatial discretizations are required. However, both models result in similar computational time for equivalent accuracy, pointing out that the distinguishing factor is the linearity of the optimisation problem.

To test the controlling capability of the proposed MPC methodology, two test cases with different maximum allowable stresses in the steam drum were studied. The stress limit in the first case assumed maximum stresses according to the utilization of modern alloys, whilst the second test case imposed tight limits on the maximum stress to ensure that this limit was reached. The MPC strategy with stress monitoring was able to compute the optimal control actions without exceeding the imposed constraints. The gas turbine ramp rate limited the operation in the first case as the stress limits were not reached. In the second test, the constraint on the effective stress was active during a period of time. These two studies demonstrate the suitability of the proposed MPC strategy to optimally control flexible NGCC with stress monitoring.

Low stress limits reduce the power generation flexibility of the NGCC. When the maximum allowable stress was reached, the control strategy decreased the gas turbine load ramps to ensure that larger temperature gradients did not arise. As a result, the load change required more time compared to the test case where stress limits for modern alloys were considered.

Temperature control was also accomplished with the MPC methodology, limiting the maximum temperature variation to below 5 °C. Lower stress limits eased the control of the superheated and reheated steam temperature. Since lower maximum allowable stress constraints lead to slower ramp rates, the temperature fluctuation in the steam was reduced.

This work proposes a optimal control methodology with both linear and nonlinear formulations for control of flexible thermal power plants with stress monitoring. Overall, this study demonstrates that (1) MPC is an adequate control strategy to include stress monitoring; (2) both linear and nonlinear formulations can limit the maximum effective stress in different components, and thus the proposed methodology can be applied to any geometry (e.g. turbine blades and rotor, steam turbine casings, piping, headers) and power system; and (3) the linear formulation shows superior computational performance and should be preferred over the nonlinear case if linear stress models are available. Furthermore, the proposed MPC methodology with stress monitoring can be applied to start-ups and shut-downs, as these are procedures where large stresses arise owing to the large temperature gradients.

Acknowledgements

This work has been financially supported by the Department of Energy and Process Engineering at the Norwegian University of Science and Technology - NTNU. The authors thank Dr. Rubén Mocholí Montañés for providing the dynamic model of the power plant and for his valuable advice.

References

[1] IPCC, Climate Change 2014: Synthesis Report, Contribution of Working Groups I, II and III to the Fifth Assessment Report of the Intergovernmental Panel on Climate Change [Core Writing Team, R.K. Pachauri and L.A. Meyer (eds.)], IPCC, Geneva, Switzerland; 2014.

[2] IPCC, Summary for Policymakers. In: Global warming of 1.5 C. An IPCC Special Report on the impacts of global warming of 1.5 C above pre-industrial levels and related global greenhouse gas emission pathways, in the context of strengthening the global response to the threat of climate change, sustainable development, and efforts to eradicate poverty, [Masson-Delmotte V, Zhai P, Pörtner HO, Roberts D, Skea J, Shukla PR, et al., editors]. World Meteorological Organization, Geneva, Switzerland; 2018.

[3] International Energy Agency - IEA, World Energy Outlook 2018: Executive Summary, <https://webstore.iea.org/download/summary/190?fileName=English-WEO-2018-ES.pdf>; 2018.

[4] European Commission, Energy Roadmap 2050. <https://eur-lex.europa.eu/LexUriServ/LexUriServ.do?uri=COM:2011:0885:FIN:EN:PDF>; 2011.

[5] Heuberger CF, Rubin ES, Staffell I, Shah N, Mac Dowell N. Power capacity expansion planning considering endogenous technology cost learning. Appl Energy 2017;204:831–45.

[6] Bertsch J, Growitsch C, Lorenczik S, Nagl S. Flexibility in Europe's power sector: an additional requirement or an automatic complement? Energy Econ 2016;53:118–31.

[7] Huber M, Dimkova D, Hamacher T. Integration of wind and solar power in Europe: assessment of flexibility requirements. Energy 2014;69:236–46.

[8] Kondziella H, Bruckner T. Flexibility requirements of renewable energy based electricity systems–a review of research results and methodologies. Renew Sustain Energy Rev 2016;53:10–22.

[9] Monta nés RM, Korpås M, Nord LO, Jaehnert S. Identifying operational requirements for flexible CCS power plant in future energy systems. Energy Proc 2016;86:22–31.

[10] Eser P, Chokani N, Abhari R. Operational and financial performance of fossil fuel power plants within a high renewable energy mix. J Global Power Propul Soc

2017;1:16–27.
[11] González-Salazar MA, Kirsten T, Prchlik L. Review of the operational flexibility and emissions of gas-and coal-fired power plants in a future with growing renewables. Renew Sustain Energy Rev 2017;82:1497–513.
[12] IEACCC - International Energy Agency Clean Coal Centre, Power plant design and managment for unit cycling, <https://www.iea-coal.org/>; 2019.
[13] Hentschel J, Spliethoff H, et al. A parametric approach for the valuation of power plant flexibility options. Energy Rep 2016;2:40–7.
[14] Alobaid F, Mertens N, Starkloff R, Lanz T, Heinze C, Epple B. Progress in dynamic simulation of thermal power plants. Prog Energy Combust Sci 2017;59:79–162.
[15] Rúa J, Agromayor R, Hillestad M, Nord LO. Optimal dynamic operation of natural gas combined cycles accounting for stresses in thick-walled components. Appl Therm Eng 2020;114858.
[16] Kim T, Lee D, Ro S. Analysis of thermal stress evolution in the steam drum during start-up of a heat recovery steam generator. Appl Therm Eng 2000;20(11):977–92.
[17] Alobaid F, Postler R, Ströhle J, Epple B, Kim H-G. Modeling and investigation start-up procedures of a combined cycle power plant. Appl Energy 2008;85(12):1173–89.
[18] Gülen SC, Kim K. Gas turbine combined cycle dynamic simulation: a physics based simple approach. J Eng Gas Turb Power 2014;136(1):011601.
[19] Taler J, Dzierwa P, Taler D, Harchut P. Optimization of the boiler start-up taking into account thermal stresses. Energy 2015;92:160–70.
[20] Taler J, Weglowski B, Taler D, Sobota T, Dzierwa P, Trojan M, et al. Determination of start-up curves for a boiler with natural circulation based on the analysis of stress distribution in critical pressure components. Energy 2015;92:153–9.
[21] Bausa J, Tsatsaronis G. Dynamic optimization of startup and load-increasing processes in power plants - Part I: method. J Eng Gas Turb Power 2001;123(1):246–50.
[22] Bausa J, Tsatsaronis G. Dynamic optimization of startup and load-increasing processes in power plants - Part II: application. J Eng Gas Turb Power 2001;123(1):251–4.
[23] Shirakawa M, Nakamoto M, Hosaka S. Dynamic simulation and optimization of start-up processes in combined cycle power plants. JSME Int J Ser B Fluids Therm Eng 2005;48(1):122–8.
[24] Albanesi C, Bossi M, Magni L, Paderno J, Pretolani F, Kuehl P, et al. Optimization of the start-up procedure of a combined cycle power plant. In: Decision and control, 2006 45th IEEE Conference on, IEEE; 2006. p. 1840–45.
[25] Prasad G, Swidenbank E, Hogg B. A local model networks based multivariable long-range predictive control strategy for thermal power plants. Automatica 1998;34(10):1185–204.
[26] Prasad G, Swidenbank E, Hogg B. A neural net model-based multivariable long-range predictive control strategy applied in thermal power plant control. IEEE Trans Energy Convers 1998;13(2):176–82.
[27] Peng H, Ozaki T, Toyoda Y, Oda K. Exponential ARX model-based long-range predictive control strategy for power plants. Control Eng Pract 2001;9(12):1353–60.
[28] Peng H, Wu J, Inoussa G, Deng Q, Nakano K. Nonlinear system modeling and predictive control using the RBF nets-based quasi-linear ARX model. Control Eng Pract 2009;17(1):59–66.
[29] Lu S, Hogg BW. Predictive co-ordinated control for power-plant steam pressure and power output. Control Eng Pract 1997;5(1):79–84.
[30] Sindareh-Esfahani P, Tabatabaei SS, Pieper JK. Model predictive control of a heat recovery steam generator during cold start-up operation using piecewise linear models. Appl Therm Eng 2017;119:516–29.
[31] Kehlhofer R, Hannemann F, Rukes B, Stirnimann F. Combined-cycle gas & steam turbine power plants. Pennwell Books; 2009.
[32] Thermoflow, GT PRO 24.0, Thermoflow Inc.
[33] Modelon, Thermal Power Library, <https://www.modelon.com/library/thermal-power-library/>.
[34] Dassault Systemes, <https://www.3ds.com/products-services/catia/products/dymola/>.
[35] Modelica Association, <https://www.modelica.org/>.
[36] Monta nés RM, GarDarsdóttir SÓ, Normann F, Johnsson F, Nord LO. Demonstrating load-change transient performance of a commercial-scale natural gas combined cycle power plant with post-combustion CO2 capture. Int J Greenhouse Gas Control 2017;63:158–74.
[37] Ljung L. System identification: theory for the user. Prentice-hall; 1987.
[38] Johansen TA, Foss B. Constructing NARMAX models using ARMAX models. Int J Control 1993;58(5):1125–53.
[39] Gevers M, Ljung L. Optimal experiment designs with respect to the intended model application. Automatica 1986;22(5):543–54.
[40] Gevers M. Identification for control: from the early achievements to the revival of experiment design. Eur J Control 2005;11:1–18.
[41] Gevers M, Mišković L, Bonvin D, Karimi A. Identification of multi-input systems: variance analysis and input design issues. Automatica 2006;42(4):559–72.
[42] Mišković L, Karimi A, Bonvin D, Gevers M. Closed-loop identification of multivariable systems: with or without excitation of all references? Automatica 2008;44(8):2048–56.
[43] Timoshenko S, Goodier JN. Theory of elasticity. McGraw-Hill book Company; 1951.
[44] ANSYS, ANSYS Academic Research Thermal and Mechanical, Release 19.2, ANSYS Inc.
[45] Jonshagen K, Genrup M. Improved load control for a steam cycle combined heat and power plant. Energy 2010;35(4):1694–700.
[46] Aske EMB, Skogestad S. Consistent inventory control. Industr Eng Chem Res 2009;48(24):10892–902.
[47] Viswanathan R, Bakker W. Materials for ultrasupercritical coal power plants - turbine materials: Part II. J Mater Eng Perform 2001;10(1):96–101.